

Electrochemical transformations of metals, metal compounds, and metal complexes: invariably (ligand/solvent)-centered

Donald T. Sawyer

Department of Chemistry, Texas A&M University, 1545 Player Drive, Lexington, KY 40511-2303, USA

Received 12 June 2002; received in revised form 22 August 2002; accepted 22 August 2002

Abstract

All reactions, and particularly redox processes, occur via the lowest-energy pathway that is available (mechanistically feasible) to the system. Metal electrodes are transformed anodically via electron removal from (a) solvent molecules [e.g. $\text{Ag}(\text{s}) + 6\text{H}_2\text{O} - \text{e}^- \rightarrow \text{Ag}^{\text{I}}(\text{OH}_2)_6^+$]; (b) electrolyte anions [e.g. $\text{Ag}(\text{s}) + \text{Cl}^- - \text{e}^- \rightarrow \text{Ag}^{\text{I}}\text{Cl}(\text{s})$]; or (c) Lewis-base ligands [e.g. $\text{Ag}(\text{s}) + 4\text{NH}_3 - \text{e}^- \rightarrow \text{Ag}^{\text{I}}(\text{NH}_3)_4^+$]. The same is true for reduced transition-metal complexes [e.g. $\text{Fe}^{\text{II}}(\text{bpy})_3^{2+} - \text{e}^- \rightarrow \text{Fe}^{\text{III}}(\text{bpy})_3^{3+}$; ligand-centered oxidation]. In the absence of ligands, most oxidations are mediated (catalyzed) via the electron-transfer transformation of water to protonated-hydroxyl radicals ($\text{H}_2^+\text{O}^\bullet$), which couple with metal (or unsaturated carbon) centers to form covalent bonds [e.g. $\text{Ag}(\text{s}) + 6\text{H}_2\text{O} - \text{e}^- \rightarrow \text{Ag}^{\text{I}}(\text{OH}_2)_6^+ \rightarrow \text{Ag}^{\text{I}}\text{-OH}(\text{s}) + \text{H}_{11}^+\text{O}_5$]. Most reductions are mediated (catalyzed) via the electron-transfer transformation of water (or hydronium ion) to hydrogen atoms (H^\bullet), which couple with unsaturated centers (or functional groups; e.g. $-\text{OH}$) of the substrate molecules to form covalent bonds; e.g. H-OH in the case of $\text{Ag}^{\text{I}}\text{-OH}$ to produce silver metal. The oxidation of metal electrodes involves electron removal (within the interface) from a solvent molecule or basic constituent (ligand) rather than from the valence-electron shell of the metal [e.g. $\text{Ag}(\text{s}) + \text{Cl}^- - \text{e}^- \rightarrow \text{Ag-Cl}(\text{s})$, $E^\circ = +0.22 \text{ V}$ versus NHE; $\text{Cl}^- - \text{e}^- \rightarrow [\text{Cl}^\bullet]$, $E^\circ = +2.47 \text{ V}$]. The difference in oxidation potential for the free ligand in the absence of the metal electrode and in its presence is a measure of the metal–ligand differential bond energy [e.g. for $\text{Ag-Cl}(\text{s})$, $\Delta(-\Delta G_{\text{BF}}) = -\Delta E^\circ \times 23.06 \text{ kcal}(\text{eV})^{-1} = 51.9 \text{ kcal mol}^{-1}$].

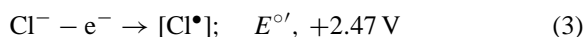
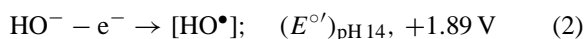
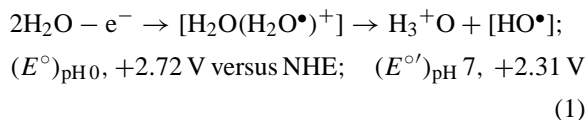
© 2002 Elsevier Science B.V. All rights reserved.

Keywords: Electrochemical transformations; Molecule; Metal complexes; Ligand-centered oxidations

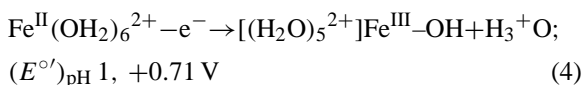
1. Introduction

Electrochemistry involves electron transfer across a solution/electrode interface [1]. At the cathode electrons (from the electrode) are transformed within the interface via reaction with ions or molecules to produce reduced molecules or ions {e.g. $\text{H}_3^+\text{O} + \text{e}^- \rightarrow [\text{H}^\bullet] + \text{H}_2\text{O}$; $\text{H}_2\text{O} + \text{e}^- \rightarrow [\text{H}^\bullet] + \text{HO}^-$; $\text{O}_2 + \text{e}^- \rightarrow \text{O}^-$; $\text{Cu}^{\text{II}}(\text{bpy})_2^{2+} + \text{e}^- \rightarrow \text{Cu}^{\text{I}}(\text{bpy})_2^+$; $\text{Fe}^{\text{III}}\text{Cl}_3 + \text{e}^- \rightarrow \text{Fe}^{\text{II}}\text{Cl}_3^-$ }. At the anode molecules or ions

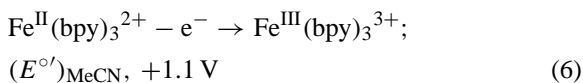
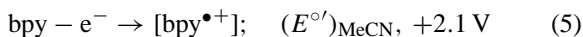
(from the solution) are transformed within the interface (inner double layer) to produce electrons (at the electrode surface) and oxidized ions and molecules. For example [1],



E-mail address: sawyer@mail.chem.tamu.edu (D.T. Sawyer).



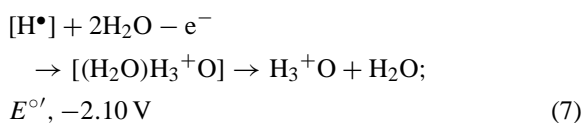
note that the roman numeral superscripts represent the number of covalent bonds, not the charge-state of the metal.



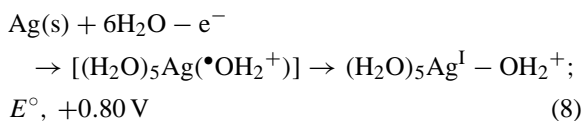
In the last example, the electron that is removed from the $\text{Fe}^{\text{II}}(\text{bpy})_3^{2+}$ comes from the ligands to give a $[\text{bpy}^{\bullet+}]$ that couples with one of the four non-bonding electrons of the iron(II) center ($d^6\text{sp}$; $S = 0$ to give a third covalent bond $[\text{Fe}^{\text{III}}(\text{bpy})_3^{3+}$; $d^5\text{sp}^2$, $S = 1/2$). The potential required to remove an electron from the $d^6\text{sp}$ manifold of the iron(II) center of $\text{Fe}^{\text{II}}(\text{OH}_2)_6^{2+}$ or $\text{Fe}^{\text{II}}(\text{bpy})_3^{2+}$ is greater than the first ionization potential of iron (7.9 eV) [2].

In the gas-phase, electron removal from atoms is limited by their ionization potential (e.g. H^\bullet , 13.6 eV; K^\bullet , 4.3 eV; Na^\bullet , 5.1 eV; Cu^\bullet , 7.7 eV, 20.3 eV; Ag^\bullet , 7.6 eV; Fe, 7.9, 16.2, 30.7 eV) [2]. However, in the solution-phase electron removal (oxidation) from the solvent may be facilitated by the presence of substrate atoms (rather than be from them).

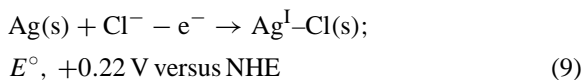
For example, with pH 0 water the process of Eq. (1) is shifted -4.82 V when hydrogen atoms are present



and -1.92 V with a silver electrode



Likewise, the oxidation of Cl^- (Eq. (3)) is facilitated at a silver electrode via formation of a $\text{Ag}^{\text{I}}-\text{Cl}$ covalent bond.

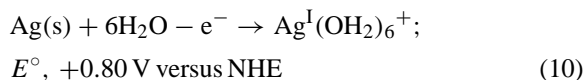


2. Metals

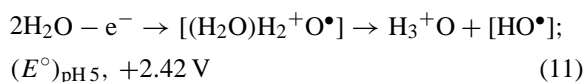
The transformation of metal-electrode surfaces via electro-oxidation to their metallo-oxides, solvated ions, and metal complexes is fundamental to most anodic electrochemical processes (batteries, electro-refining, anodic-stripping analysis, and reference electrodes). Although this is traditionally represented as the removal of one (or more) valence electrons from a metal atom at the electrode surface to give a metal ion [e.g. $\text{Ag}(\text{s}) - e^- \rightarrow \text{Ag}^+$; E° , $+0.80 \text{ V}$ versus NHE], the gas-phase ionization potential [e.g. $\text{Ag}^\bullet(\text{g}) - e^- \rightarrow \text{Ag}^+(\text{g})$; IP, 7.6 eV] is far greater than the observed oxidation potential [2]. The difference is attributed to the solvation energy for the metal ion [e.g. $\text{Ag}^+ + n\text{H}_2\text{O} \rightarrow \text{Ag}^+(\text{aq})$; $-\Delta G(\text{aq}) \approx 70\text{--}100 \text{ kcal mol}^{-1}$]. However, such a sequential path would not obviate the 7.6 V energy barrier for the initial step and is in conflict with the observed thermodynamic reversibility for many metal/solvated-metal-ion redox couples.

All reactions, and particularly redox processes, occur via the easiest and lowest-energy pathway that is available (mechanistically feasible) to the system. In the case of a metal-electrode/electrolyte interface undergoing anodic transformations, the electrons can come from (a) surface metal atoms (energy limit; first ionization potential), (b) solvent molecules (energy limit; oxidation potential of solvent), (c) electrolyte anions (energy limit; oxidation potential of anions), and (d) base-ligands (energy limit; oxidation potential of ligand). All metal electrodes are electrochemically transformed via path (b), (c), or (d), and never via path (a). This general conclusion is illustrated for silver and copper electrodes in aqueous and acetonitrile (MeCN) solutions that contain inert electrolyte, chloride ion (Cl^-), or bipyridine (bpy).

In aqueous solutions at pH 5, the silver electrode facilitates oxidation of water



In contrast to the silver atoms of $\text{Ag}(\text{s})$ (ionization potential $>7.6 \text{ eV}$), water is oxidized (gives up an electron) at much lower potentials



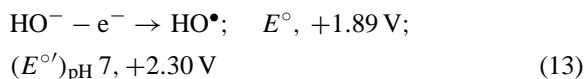
At a silver electrode the latter process is facilitated via formation of a $\text{Ag}^{\text{I}}\text{-OH}_2^+$ bond; the shift in oxidation potential from +2.42 to +0.80 V is a measure of the differential bond-formation energy $\Delta(-\Delta G_{\text{BF}})$ [difference in the bond energy for a silver atom in $\text{Ag}^{\text{I}}\text{-OH}_2^+(\text{OH}_2)_5$ and in the solid metal matrix ($1/n\text{Ag}_n \rightarrow [\text{Ag}^\bullet](\text{g}); \Delta H_{\text{esc}} = 68 \text{ kcal mol}^{-1}$)] [3]

$$\begin{aligned} \Delta(-\Delta G_{\text{BF}}) &= (+2.42 - 0.80) \times 23.06 \\ &= 37.4 \text{ kcal mol}^{-1} \end{aligned} \quad (12)$$

Hence, addition of the escape energy (ΔH_{esc} , energy required to release a mole of elemental atoms from the standard state) to the differential bond-formation energy gives the free energy of bond formation for the silver-hydrate ion $\{[\text{Ag}^\bullet] + [(\text{H}_2\text{O})_5(\text{H}_2^+\text{O}^\bullet)] \rightarrow \text{Ag}^{\text{I}}(\text{OH}_2)_6^+; -\Delta G_{\text{BF}}(\text{aq}) = 37.4 + 68 = 105 \text{ kcal mol}^{-1}\}$. Combination of the differential bond-forma-

tion energy for any metal-hydrate ion $[\text{M}(\text{OH}_2)_m^{n+}]$ [$\Delta(-\Delta G_{\text{BF}}) = (+2.42 - E_{\text{M}}^\circ)23.06$] with the metal's escape energy (ΔH_{esc}) provides a measure of its free energy for metal-hydrate bond formation {e.g. $[\text{M}^\bullet] + [(\text{H}_2\text{O})_5(\text{H}_2^+\text{O}^\bullet)] \rightarrow \text{M}^{\text{I}}(\text{OH}_2)_6^+; -\Delta G_{\text{BF}}(\text{aq})$ }. Table 1 summarizes such evaluations for a number of metal-hydrate ions.

At pH 14, the anodic process for water is the oxidation of HO^-



which at a silver electrode is facilitated via formation of a $\text{Ag}^{\text{I}}\text{-OH}$ bond [$\Delta(-\Delta G_{\text{BF}}) = (1.89 - 0.34) \times 23.06 = 35.7 \text{ kcal mol}^{-1}$] [1]

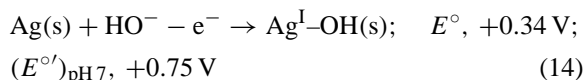


Table 1

Free-energy of bond formation [$-\Delta G_{\text{BF}}(\text{aq})$] for metal-hydrate ions [e.g. $\text{M}^\bullet + (\text{H}_2\text{O})_5(\text{H}_2^+\text{O}^\bullet) \rightarrow \text{M}^{\text{I}}(\text{OH}_2)_6^+, -\Delta G_{\text{BF}}(\text{aq})_{\text{pH } 5}$]^a

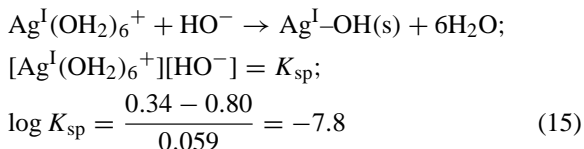
Reduction half-reaction	$E^{\circ\text{b}}$ (V vs. NHE)	$\Delta(-\Delta(G^{\circ})'_{\text{BF}})^{\text{c}}$ (kcal mol ⁻¹)	$\Delta H_{\text{esc}}^{\text{c}}$ (kcal mol ⁻¹)	$-\Delta G_{\text{BF}}(\text{aq})$ (kcal mol ⁻¹)
$\text{Li}^{\text{I}}(\text{OH}_2)_6^+ + e^- = \text{Li}(\text{s}) + 6\text{H}_2\text{O}$	-3.04	126	39	165
$\text{K}^{\text{I}}(\text{OH}_2)_6^+ + e^- = \text{K}(\text{s}) + 6\text{H}_2\text{O}$	-2.92	123	21	144
$\text{Ca}^{\text{II}}(\text{OH}_2)_6^{2+} + 2e^- = \text{Ca}(\text{s}) + 6\text{H}_2\text{O}$	-2.84	243	43	2 × 143
$\text{Na}^{\text{I}}(\text{OH}_2)_6^+ + e^- = \text{Na}(\text{s}) + 6\text{H}_2\text{O}$	-2.71	118	26	144
$\text{Mg}^{\text{II}}(\text{OH}_2)_6^{2+} + 2e^- = \text{Mg}(\text{s}) + 6\text{H}_2\text{O}$	-2.36	221	35	2 × 128
$\text{Al}^{\text{III}}(\text{OH}_2)_6^{3+} + 3e^- = \text{Al}(\text{s}) + 6\text{H}_2\text{O}$	-1.67	284	79	3 × 121
$\text{Mn}^{\text{II}}(\text{OH}_2)_6^{2+} + 2e^- = \text{Mn}(\text{s}) + 6\text{H}_2\text{O}$	-1.18	166	68	2 × 117
$\text{Cr}^{\text{II}}(\text{OH}_2)_6^{2+} + 2e^- = \text{Cr}(\text{s}) + 6\text{H}_2\text{O}$	-0.90	154	95	2 × 124
$\text{Zn}^{\text{II}}(\text{OH}_2)_6^{2+} + 2e^- = \text{Zn}(\text{s}) + 6\text{H}_2\text{O}$	-0.76	147	31	2 × 89
$\text{Fe}^{\text{II}}(\text{OH}_2)_6^{2+} + 2e^- = \text{Fe}(\text{s}) + 6\text{H}_2\text{O}$	-0.44	132	35	2 × 84
$\text{Cd}^{\text{II}}(\text{OH}_2)_6^{2+} + 2e^- = \text{Cd}(\text{s}) + 6\text{H}_2\text{O}$	-0.40	130	27	2 × 79
$\text{Co}^{\text{II}}(\text{OH}_2)_6^{2+} + 2e^- = \text{Co}(\text{s}) + 6\text{H}_2\text{O}$	-0.28	125	102	2 × 114
$\text{Ni}^{\text{II}}(\text{OH}_2)_6^{2+} + 2e^- = \text{Ni}(\text{s}) + 6\text{H}_2\text{O}$	-0.26	124	103	2 × 114
$\text{Pb}^{\text{II}}(\text{OH}_2)_6^{2+} + 2e^- = \text{Pb}(\text{s}) + 6\text{H}_2\text{O}$	-0.13	118	47	2 × 83
$\text{H}_{13}^+\text{O}_6 + e^- = (1/2)\text{H}_2(\text{g}) + 6\text{H}_2\text{O}$	0.00 (pH 0)	63	52	115
$\text{Cu}^{\text{II}}(\text{OH}_2)_6^{2+} + 2e^- = \text{Cu}(\text{s}) + 6\text{H}_2\text{O}$	+0.34	96	81	2 × 89
$\text{Cu}^{\text{I}}(\text{OH}_2)_6^+ + e^- = \text{Cu}(\text{s}) + 6\text{H}_2\text{O}$	+0.52	44	81	125
$\text{Ag}^{\text{I}}(\text{OH}_2)_6^+ + e^- = \text{Ag}(\text{s}) + 6\text{H}_2\text{O}$	+0.80	37	68	105
$\text{Hg}^{\text{II}}(\text{OH}_2)_6^{2+} + 2e^- = \text{Hg}(\text{s}) + 6\text{H}_2\text{O}$	+0.85	73	15	2 × 44
$\text{Pd}^{\text{II}}(\text{OH}_2)_6^{2+} + 2e^- = \text{Pd}(\text{s}) + 6\text{H}_2\text{O}$	+0.91	70	90	2 × 80
$\text{Pt}^{\text{II}}(\text{OH}_2)_6^{2+} + 2e^- = \text{Pt}(\text{s}) + 6\text{H}_2\text{O}$	+1.19	57	135	2 × 96
$\text{Au}^{\text{III}}(\text{OH}_2)_6^{3+} + 3e^- = \text{Au}(\text{s}) + 6\text{H}_2\text{O}$	+1.52	63	80	3 × 48
$\text{Au}^{\text{I}}(\text{OH}_2)_6^+ + e^- = \text{Au}(\text{s}) + 6\text{H}_2\text{O}$	+1.83	14	80	94
$(\text{H}_2\text{O})_5(\text{H}_2^+\text{O}^\bullet) + e^- = 6\text{H}_2\text{O}$	+2.72 (pH 0), +2.42 (pH 5)			

^a $\Delta G_{\text{BF}}(\text{aq}) = \Delta(-\Delta(G^{\circ})'_{\text{BF}}) + \Delta H_{\text{esc}} = ((E^{\circ})'_{\text{HO}^\bullet/\text{H}_2\text{O}} - E_{\text{M}^+/ \text{M}}^\circ)_{\text{pH } 5} \times 23.06 + \Delta H_{\text{esc}}$.

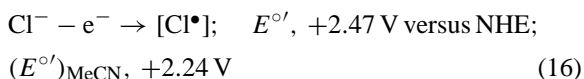
^b [1,4].

^c [3].

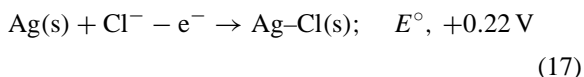
Hence, the homolytic bond-formation free energy is the sum of $\Delta(-\Delta G_{\text{BF}})$ and $\Delta H_{\text{esc}}\{[\text{Ag}^\bullet] + [\text{HO}^\bullet] \rightarrow \text{Ag}-\text{OH}(\text{s}); -\Delta G_{\text{BF}} = 36 + 68 = 104 \text{ kcal mol}^{-1}\}$. The data of Eqs. (10) and (14) can be combined to give a value for the solubility product (K_{sp}) for Ag–OH(s)



In the presence of chloride ion, metal electrodes facilitate its oxidation



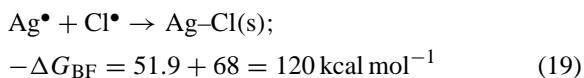
via formation of metal–chlorine covalent bonds, e.g.



Hence, the differential bond-formation energy [$\Delta(-\Delta G_{\text{BF}})$] (Ag–Cl bond energy, minus the energy required to break the bonds of a silver atom at the Ag(s) surface is given by the difference in oxidation potentials (Eqs. (16) and (17))

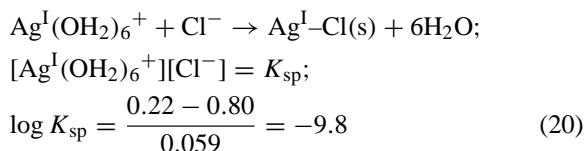
$$\begin{aligned} \Delta(-\Delta G_{\text{BF}}) &= (2.47 - 0.22) \times 23.06 \\ &= 51.9 \text{ kcal mol}^{-1} \end{aligned} \quad (18)$$

The escape energy for a $[\text{Ag}^\bullet]$ atom from Ag(s) is 68 kcal mol⁻¹ [3]. When combined with Eq. (18), this gives a reasonable value for $-\Delta G_{\text{BF}}$

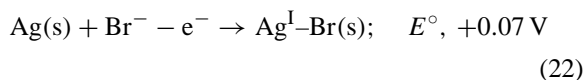
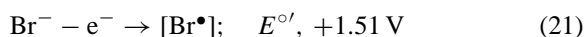


The literature value for the dissociative bond energy (ΔH_{DBE}) of Ag–Cl(g) is 81.6 kcal mol⁻¹, which is equivalent to an estimated $-\Delta G_{\text{BF}}$ value of 73.8 kcal mol⁻¹ [$-\Delta G_{\text{BF}} = \Delta H_{\text{DBE}} - T\Delta S = 81.6 - 7.8(\text{est}) = 73.8 \text{ kcal mol}^{-1}$] [3]. The energy to vaporize AgCl(s) (ΔG_{vap} , 42 kcal mol⁻¹) [4], when added to the gas-phase formation energy ($-\Delta G_{\text{BF}}$), gives a literature value of 116 kcal mol⁻¹ for ($-\Delta G_{\text{BF}}$); within experimental error of the electrochemical evaluation (Eq. (19)). Thus, the proposition that metal-electrode oxidations are solvent or

ligand-centered with potentials that reflect the metal–solvent/ligand bond-formation free energies ($-\Delta G_{\text{BF}}$) is supported by independent bond-energy data. The data of Eqs. (10) and (17) provide a measure of the solubility product for AgCl(s).



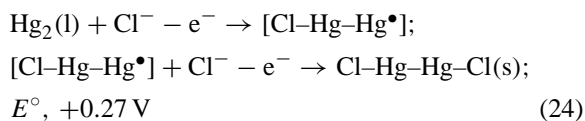
Similar results are observed for a silver electrode in the presence of Br⁻



which gives a measure of the Ag^I–Br bond energy

$$\begin{aligned} \Delta(-\Delta G_{\text{BF}}) &= (1.51 - 0.07) \times 23.06 \\ &= 33.1 \text{ kcal mol}^{-1} \end{aligned} \quad (23)$$

Another important example is the oxidation of Cl⁻ at a mercury electrode [Hg₂(l)] to form calomel [mercurous chloride, Hg₂Cl₂(s), Cl–Hg^{II}–Hg^{II}–Cl(s)].



The potential shift for the Cl⁻/Cl[•] couple from +2.47 V (Eq. (16)) to +0.27 V in the presence of Hg₂(l) is a measure of the [Cl–HgHg] bond energy [$-\Delta G_{\text{BF}} = (2.47 - 0.27) \times 23.06 = 50.7 \text{ kcal mol}^{-1}$].

Similar metal-facilitated oxidations of H₂O and of Cl⁻ occur for all metal electrodes. The respective potentials for the oxidation of each at a copper electrode are

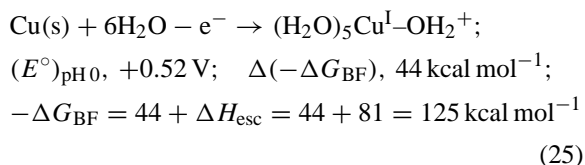


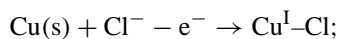
Table 2
Redox potentials (E°) for the $M^I(\text{OH}_2)_n^+/M$ and $M^I\text{OH}/M$, HO^- couples of Cu, Ag, and Au in H_2O and in MeCN (0.1 M tetraethylammonium perchlorate)

M	E° (V vs. NHE ^a)	
	$M^I(\text{solv})_n^+/M$	$M^I\text{OH}/M, \text{HO}^-$
(A) H_2O^b		
Cu	+0.52	-0.36
Ag	+0.80	+0.34
Au	+1.7	
$\text{H}_2^+\text{O}^*/\text{H}_2\text{O};$ $\text{HO}^*/\text{HO}^-(\text{GC})$	+2.72 (+2.42) _{pH5}	+1.89
(B) MeCN ^c		
Cu	+0.19	-0.79
Ag	+0.54	-0.30
Au	+1.58	-0.19
$\text{H}_2^+\text{O}^*(\text{MeCN})/\text{H}_2\text{O};$ $\text{HO}^*/\text{HO}^-(\text{GC})$	+3.2	+0.92

^a SCE = +0.244 V vs. NHE.

^b [1].

^c [5].

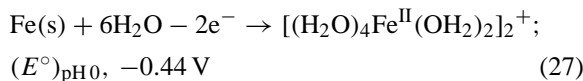


$$E^\circ, +0.14 \text{ V}; \quad \Delta(-\Delta G_{\text{BF}}), 54 \text{ kcal mol}^{-1};$$

$$-\Delta G_{\text{BF}} = 54 + \Delta H_{\text{esc}} = 54 + 81 = 135 \text{ kcal mol}^{-1} \quad (26)$$

Additional redox data for oxidations of $\text{H}_2\text{O}/\text{HO}^-$ at Cu, Ag, and Au electrodes in aqueous and acetonitrile (MeCN) solutions are summarized in Table 2 [1,5].

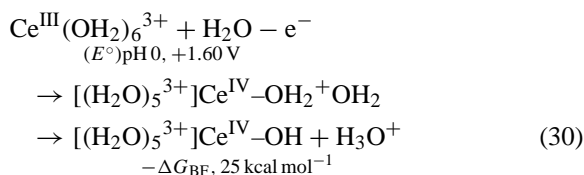
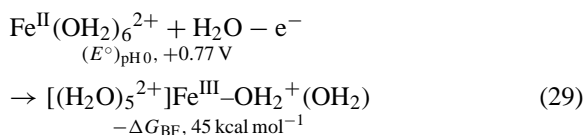
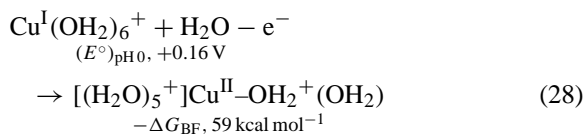
At pH 0 with an iron electrode, the water oxidation of Eq. (11) is shifted by -3.16 V,



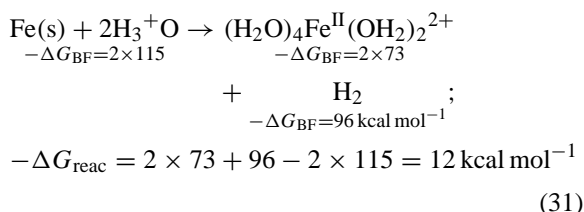
which indicates that the (H_2^+O^*) species is stabilized by a strong $[(\text{H}_2\text{O})_4(\text{H}_2\text{O})^+]\text{Fe}^{\text{II}}\text{-OH}_2^+$ covalent bond $[\Delta(-\Delta G_{\text{BF}}), \sim 73 \text{ kcal mol}^{-1}]$.

3. Metal complexes

In an analogous fashion, the removal of an electron (oxidation) from water via Eq. (11) is aided by the presence of transition-metal ions [e.g. $\text{Cu}^I(\text{OH}_2)_6^+$, $\text{Fe}^{\text{II}}(\text{OH}_2)_6^{2+}$, and $\text{Ce}^{\text{III}}(\text{OH}_2)_6^{3+}$, each with one, two, and three M-OH_2^+ covalent bonds, respectively]



In none of these examples has the potential for removal of an electron approached the ionization potentials of the metals. Although traditional treatments attribute the potentials of Eqs. (10), (25), and (27)–(30) to the removal of electrons from the metals, coupled with large ionic solvation energies, this requires a pathway with the ionization potential as a kinetic barrier. Furthermore, the spontaneous reaction of iron with acidified water is driven by the formation of Fe-OH_2^+ and H-H covalent bonds that facilitate hydrogen-atom transfer from water (rather than electron transfer from iron)



Note that to ionize a gas-phase iron atom ($\text{Fe} - 3\text{e}^- \rightarrow \text{Fe}^{3+}$) requires 54.8 eV (1266 kcal mol⁻¹); [2] in turn this species reacts upon dissolution into liquid water $\{\text{Fe}^{3+}(\text{g}) + 7\text{H}_2\text{O}(\text{l}) \rightarrow [(\text{H}_2\text{O})_5^{2+}]\text{Fe}^{\text{III}}\text{-OH} + \text{H}_3^+\text{O}, -\Delta H \approx 1000 \text{ kcal mol}^{-1}(1266 - 266)\}$; the net energy change often is ascribed as the solvation energy for $\text{Fe}^{3+}(\text{g})$ (heat of hydration).

Within an aprotic solvent (e.g. MeCN) oxidation of metals and metal complexes also is ligand-centered with the potential determined by the oxidation potential of the ligand and the metal–ligand covalent bond-formation free energy ($-\Delta G_{\text{BF}}$). For example, the free bipyridine (bpy) ligand in acetonitrile is ox-

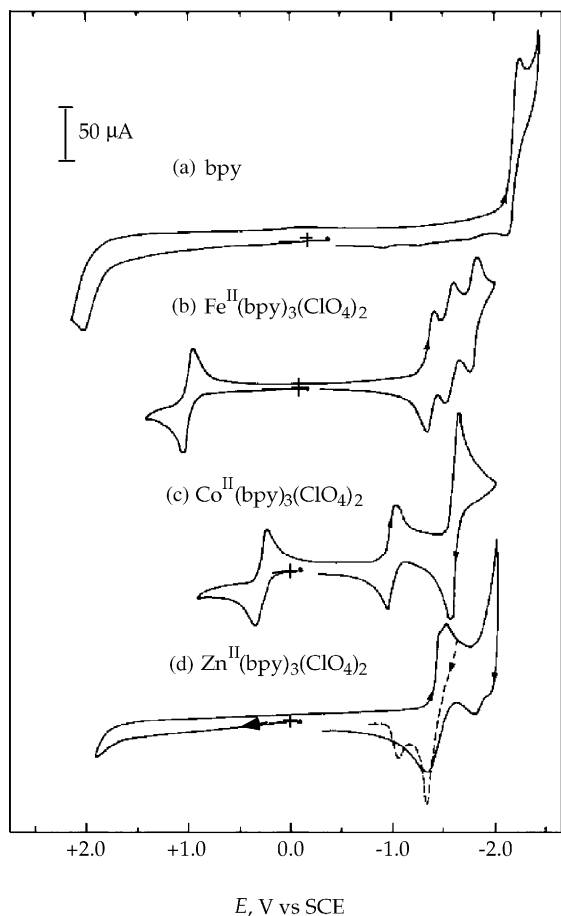
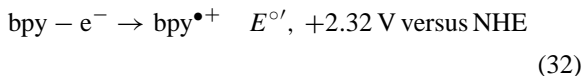
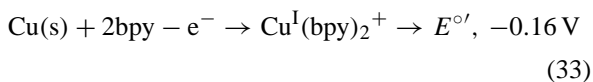


Fig. 1. Cyclic voltammograms of 3-mM solutions in MeCN (0.1 M tetraethylammonium perchlorate): (a) bpy; (b) $\text{Fe}^{\text{II}}(\text{bpy})_3^{2+}$; (c) $\text{Co}^{\text{II}}(\text{bpy})_3^{2+}$; (d) $\text{Zn}^{\text{II}}(\text{bpy})_3^{2+}$. Conditions: scan rate 0.1 V s^{-1} ; 25°C ; glassy-carbon working electrode (0.09 cm^2); SCE vs. NHE, $+0.244 \text{ V}$.

idized near the solvent limit at a glassy carbon electrode (GC) (Fig. 1) [6],

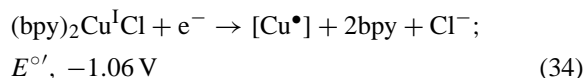


but at a copper electrode the oxidation occurs at a negative potential [7]



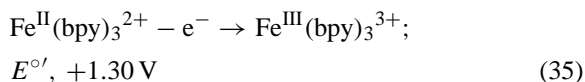
Even more striking is the reduction of $[(\text{bpy})_2\text{Cu}^{\text{I}}(\text{OH}_2)]^+$ at a glassy carbon electrode, which occurs

at -1.04 V versus NHE. The difference (-0.88 V) is due to the Cu–Cu bond energy ($20.3 \text{ kcal mol}^{-1}$) that must be overcome in the metal-oxidation process. Reduction of $(\text{bpy})_2\text{Cu}^{\text{I}}\text{Cl}$ at a glassy carbon electrode occurs at essentially the same potential as that for $\text{Cu}^{\text{I}}(\text{MeCN})_4\text{Cl}$ (-1.01 V versus NHE) [8]



The difference between this value and that for the $\text{Cl}^{\bullet}/\text{Cl}^-$ couple (Eq. (17), $+2.24 \text{ V}$ versus NHE) is a measure of the $(\text{bpy})_2\text{Cu}^{\text{I}}\text{Cl}$ bond energy $\{-\Delta G_{\text{BF}} = [2.24 - (-1.06)] \times 23.06 = 76.1 \text{ kcal mol}^{-1}$ (the value for gas-phase $\text{Cu}-\text{Cl}(\text{g})$ is $84 \pm 1 \text{ kcal mol}^{-1}$)}

Fig. 1 illustrates that the oxidation of the $\text{Fe}^{\text{II}}(\text{bpy})_3^{2+}$ complex is reversible and ligand-centered [6]



(Noteworthy are the three reversible one-electron reductions for this complex.) The electron that is removed from the $\text{Fe}^{\text{II}}(\text{bpy})_3^{2+}$ complex comes from the ligands to give $\text{bpy}^{\bullet+}$, which couples with one of the four non-bonding electrons of the iron(II) center (d^6sp) to give a third covalent bond [$\text{Fe}^{\text{III}}(\text{bpy})_3^{3+}$, d^5sp^2 ; $S = 1/2$]. The difference in oxidation potentials for $\text{Fe}^{\text{II}}(\text{bpy})_3^{2+}$ and free bpy (Eq. (32)) is a measure of the $\text{Fe}^{\text{III}}\text{--bpy}^+$ bond energy $[-\Delta G_{\text{BF}} = (2.32 - 1.30) \times 23.06 = 23.5 \text{ kcal mol}^{-1}]$. The potential that would be required to remove an electron from the d^6sp manifold of the iron(II) center of $\text{Fe}^{\text{II}}(\text{OH}_2)_6^{2+}$ or $\text{Fe}^{\text{II}}(\text{bpy})_3^{2+}$ would be greater than the first ionization potential of atomic iron (7.9 eV) [2].

Table 3 summarizes the oxidation potentials for ligands (L) and their $\text{M}^{\text{II}}\text{L}_3$ complexes with zinc(II), manganese(II), iron(II), and cobalt(II). The difference in the potentials for the free and complexed ligands is a measure of the metal(III)–ligand bond-formation energies ($-\Delta G_{\text{BF}}$); these are summarized in Table 4 [6]. For this group of complexes, the order of metal(III)–nitrogen bond energies, $\text{Co}^{\text{III}}(\text{bpy})_3^{3+} > \text{Fe}^{\text{III}}(\text{bpy})_3^{3+} > \text{Mn}^{\text{III}}(\text{bpy})_3^{3+}$, and of metal(III)–oxygen bond energies, $\text{Fe}^{\text{III}}(\text{acac})_3 > \text{Co}^{\text{III}}(\text{acac})_3 > \text{Mn}^{\text{III}}(\text{acac})_3$, is consistent with

Table 3

Oxidation potentials for ligands (L) and their ML₃ complexes with Zn(II), Mn(II), Fe(II), and Co(II) in MeCN (0.1 M tetraethylammonium perchlorate)

Ligand (L or L ⁻) ^a	<i>E</i> _{1/2} ^b (V vs. NHE) ^c				
	L/L ^{•+} (L ⁻ /L [•])	Zn ^{II} L ₃	Mn ^{II} L ₃	Fe ^{II} L ₃	Co ^{II} L ₃
H ₂ O	+2.8	+2.8	+2.8	+1.84	+2.8
bpy	+2.32	>2.5	+1.55	+1.30	+0.58
PA ⁻	+1.50	+1.54	+0.60	+0.20	+0.04
acac ⁻	+0.55	+0.58	+0.18	-0.42	-0.35
8Q ⁻	+0.21	+0.22	-0.06	-0.41	-0.57

^a Key: bpy, 2,2'-bipyridine; PA⁻, picolinate(2-carboxylate pyridine); acac⁻, acetylacetonate; 8Q⁻, 8-quinolate.

^b *E*_{1/2} taken as (*E*_{*p,a*} + *E*_{*p,c*})/2 for reversible couples of Mn^{II}L₃ and Fe^{II}L₃ complexes; as *E*_{*p,a/2*} + 0.03 V for L (or L⁻) and Zn^{II}L₃; and as *E*_{*p,c/2*} - 0.03 V for Co^{II}L₃ complex that exhibit separated redox couples.

^c SCE vs. NHE; +0.244 V.

their relative stability constants. With the picolinate (PA⁻) ligand, there is a combination of metal–oxygen covalent bonding and nitrogen–base donor interaction, which shifts the bond-energy order, Co^{III}(PA)₃ > Fe^{III}(PA)₃ > Mn^{III}(PA)₃. All of

Table 4

Apparent Metal–ligand covalent bond-formation free energies (-Δ*G*_{BF}) for several Mn, Fe, and Co complexes

Complex	-Δ <i>G</i> _{BF} (kcal mol ⁻¹) ^a
(A) Mn	
(8Q) ₂ Mn ^{III} -8Q	6
(acac) ₂ Mn ^{III} -acac	9
(PA) ₂ Mn ^{III} -PA	22
[(bpy) ₂ Mn ^{III} -bpy] ³⁺	>23 ^b
(B) Fe	
(8Q) ₂ Fe ^{III} -8Q	15
(acac) ₂ Fe ^{III} -acac	23
(PA) ₂ Fe ^{III} -PA	31
[(bpy) ₂ Fe ^{III} -bpy] ³⁺	>29 ^b
[(Ph ₃ PO) ₃ Fe ^{III} -OPPh ₃] ³⁺	>30 ^b
[(MeCN) ₄ Fe ^{III} -OH ₀] ³⁺	23
(C) Co	
(8Q) ₂ Co ^{III} -8Q	16
(acac) ₂ Co ^{III} -acac	21
(PA) ₂ Co ^{III} -PA	35
[(bpy) ₂ Co ^{III} -bpy] ³⁺	>46 ^b

^a -Δ*G*_{BF} = [*E*_{1/2}(ZnL₃⁻/ZnL₂(L[•])) - *E*_{1/2}(ML₃⁻/ML₃)] × 23.06 kcal mol⁻¹.

^b -Δ*G*_{BF} = [*E*_{*p,a*}(ZnL/ZnL^{•+}) - *E*_{*p,a*}(ML/M-L⁺)] × 23.06 kcal mol⁻¹; L = (bpy)₃ or (Ph₃PO)₄.

Table 5

Redox potentials for ligands in acetonitrile [0.1 M (Et₄N)ClO₄]

Ligand (L) ^a	<i>E</i> _{<i>p,a</i>} (V vs. SCE) ^b	<i>E</i> _{<i>p,c</i>} (V vs. SCE) ^b
H ₂ O	2.80	
py	2.30	-2.75
bpy	2.15	-2.25
tpy	2.00	-2.15, -2.5
Cl ⁻	2.00	
PhC(O)O ⁻	1.45	
PA ⁻	1.34	
AcO ⁻	1.30	
DPAH ⁻	1.20	
HOC(O)O ⁻	1.15, 1.55	
HO ⁻	0.68	
PhCH ₂ O ⁻	0.50	
DPA ²⁻	0.25, 1.25	
TDTH ⁻	-0.05	

^a Key: bpy, 2,2'-bipyridine; tpy, 2,2':6',2''-terpyridine; PA⁻, picolinate anion; DPAH⁻, 2,6-carboxyl, carboxylato-pyridine anion; DPA²⁻, 2,6-dicarboxylato-pyridine dianion; HOC(O)O⁻, bicarbonate anion; TDTH⁻, toluene-3,4-dithiol anion.

^b *E*_{*p,a*}, anodic peak potential; *E*_{*p,c*}, cathodic peak potential. Glassy carbon electrode (GCE); scan rate 0.1 V s⁻¹. Saturated calomel electrode (SCE); *E*_{SCE}, +0.244 V vs. NHE.

the data are consistent with ligand-centered redox processes.

Table 5 summarizes the oxidation potentials for a variety of ligands (L) in acetonitrile (MeCN) [1,6]. Their relative Lewis basicity (nucleophilicity) increases as their oxidation potential is less positive (or more negative). However, the potential at which L is oxidized (and L[•] is reduced) within an ML_x complex is shifted by the M–L covalent bond energy (-Δ*G*_{BF}). Figs. 2 and 3 illustrate the electrochemistry for several copper(II) and copper(I) complexes in MeCN [7,8]. The redox potentials for these copper complexes and their ligands are summarized in Table 6. In addition, the shift in redox potential (Δ*E*) for the free ligand (L) and when bonded in a complex (CuL_x) is tabulated. This quantity is a measure of the apparent copper–ligand covalent bond-formation free energy (-Δ*G*_{BF})

$$-\Delta G_{BF} = (\Delta E)23.06 \text{ kcal mol}^{-1} \quad (36)$$

Table 7 summarizes the copper–ligand bond energies for the various complexes.

The dianion of toluene-3,4-dithiol (TDT²⁻) forms unique complexes [M^{II}(TDT)₂²⁻] with transition

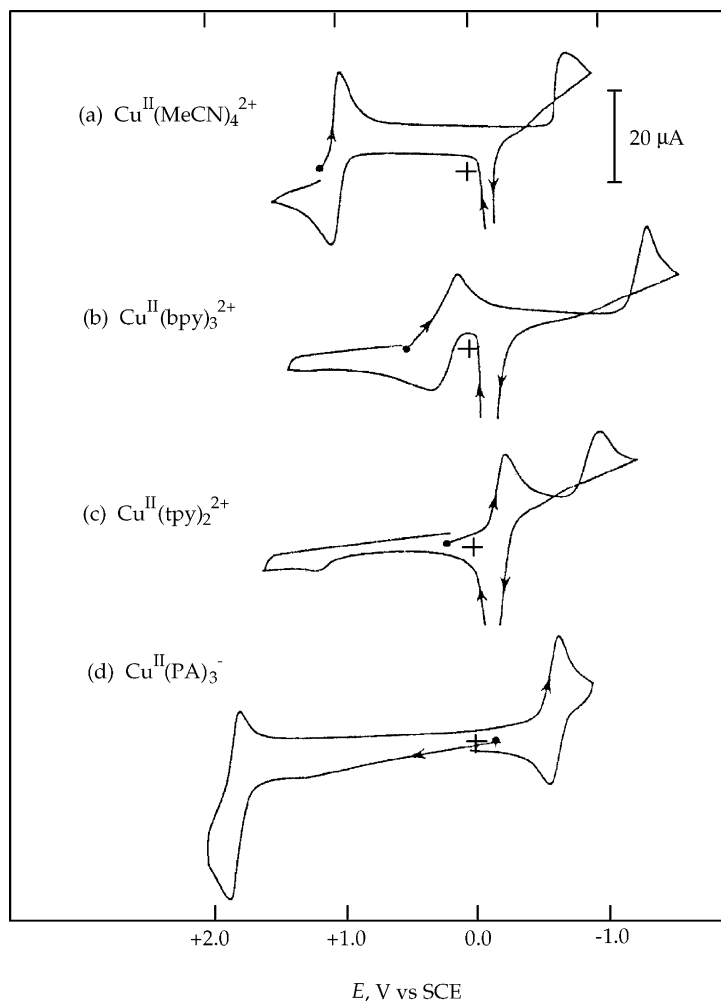


Fig. 2. Cyclic voltammograms for: (a) 1 mM $[\text{Cu}^{\text{II}}(\text{MeCN})_4](\text{ClO}_4)_2$; (b) (a) plus 3 eq. of bpy; (c) (a) plus 2 eq. of tpy; (d) (a) plus 3 eq. of PA^- in MeCN [0.1 M $(\text{Et}_4\text{N})\text{ClO}_4$]. Scan rate 0.1 V s^{-1} ; GCE (0.9 cm^2); SCE vs. NHE, $+0.244 \text{ V}$.

metals that are readily oxidized via a ligand-centered process to $\text{M}^{\text{III}}(\text{TDT})_2^-$ [9]. Fig. 4 illustrates the cyclic voltammetry for the latter complexes of Cu, Ni, Co, and Fe. Not only do each of the $\text{M}^{\text{III}}(\text{TDT})_2^-$ complexes undergo a reversible one-electron reduction, but the Ni(III), Co(III), and Fe(III) complexes also exhibit a somewhat reversible oxidation to the M(IV) valence state. For example,

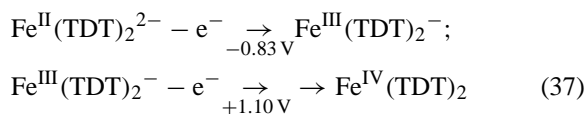


Table 8 summarizes the redox potentials for this group of complexes and the estimated M–S bond energies ($-\Delta G_{\text{BF}}$) in the $\text{M}^{\text{III}}(\text{TDT})_2^-$ and $\text{M}^{\text{IV}}(\text{TDT})_2$ complexes. These are based on the oxidation-potential difference (ΔE) between the $\text{M}^{\text{II}}(\text{TDT})_2^{2-}$ complex and $\text{Zn}^{\text{II}}(\text{TDT})_2^{2-}$ (not able to form a third covalent bond) and the ΔE between $\text{M}^{\text{III}}(\text{TDT})_2^-$ and $\text{Cu}^{\text{III}}(\text{TDT})_2^-$ (filled valence-electron shell and unable to form a fourth covalent bond), respectively [$-\Delta G_{\text{BF}} = (\Delta E)23.06 \text{ kcal mol}^{-1}$].

Although most iron(II) complexes are oxidized by hydrogen peroxide (HOOH) via Fenton chemistry,

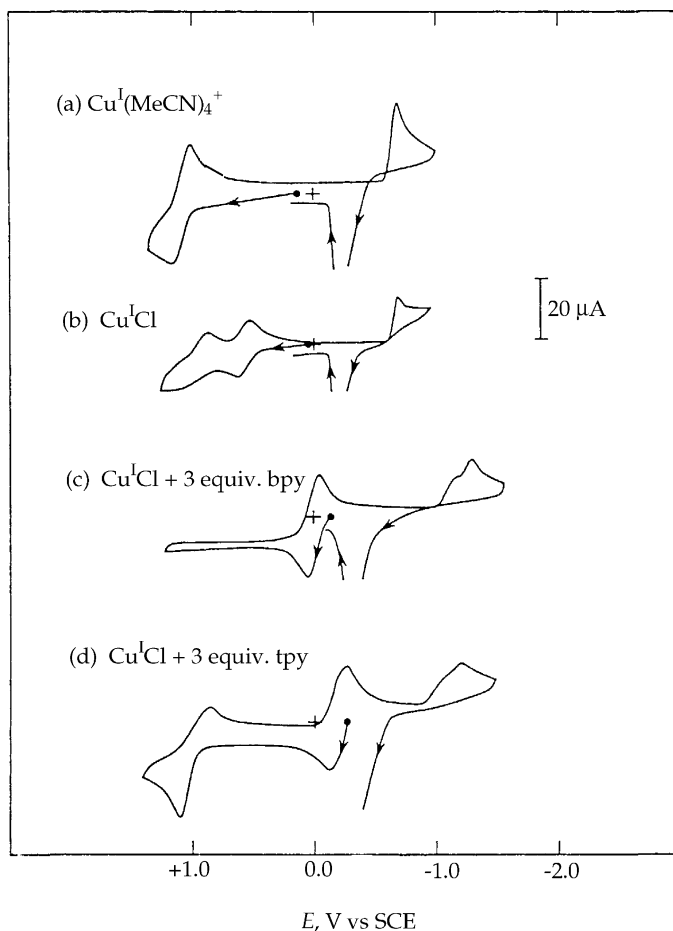
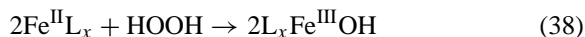
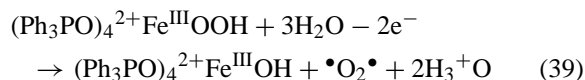


Fig. 3. Cyclic voltammograms for: (a) 1 mM $[\text{Cu}^{\text{I}}(\text{MeCN})_4(\text{ClO}_4)]$; (b) 1 mM $\text{Cu}^{\text{I}}\text{Cl}$; (c) (b) plus 3 mM bpy; (d) (b) plus 3 mM tpy in MeCN [0.1 M $(\text{Et}_4\text{N})\text{ClO}_4$]. Scan rate 0.1 V s^{-1} ; GCE (0.09 cm^2); SCE vs. NHE, $+0.244 \text{ V}$.



within MeCN the combination of $\text{Fe}^{\text{II}}(\text{OPPh}_3)_4^{2+}$ and HOOH (1:10) yields a unique purple complex [λ_{max} , 576 nm ($\epsilon = 1770 \text{ M}^{-1} \text{ s}^{-1}$)], $[(\text{Ph}_3\text{PO})_4^{2+}]\text{Fe}^{\text{III}}\text{OOH}$ [10]. The reversible one-electron, ligand-centered oxidation of $\text{Fe}^{\text{II}}(\text{OPPh}_3)_4^{2+}$ at $+1.2 \text{ V}$ versus SCE is replaced by an irreversible two-electron oxidation at $+1.9 \text{ V}$ (Fig. 5)



Whereas $\text{Fe}^{\text{II}}(\text{OPPh}_3)_4^{2+}$ is reduced by two electrons at -1.1 V to give metallic iron, the $(\text{Ph}_3\text{PO})_4^{2+}\text{Fe}^{\text{III}}\text{OOH}$ complex is reduced in several steps to give an iron oxide

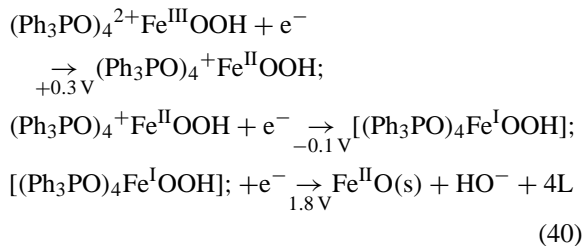


Table 6
Redox potentials for copper complexes and their ligands in MeCN

Electrode reaction	$E_{1/2}^a$ (V vs. SCE ^b)	ΔE^c (V)
$\text{bpy} - e^- \rightarrow \text{bpy}^{\bullet+}$	2.1	
$\text{Cu}^{\text{II}}(\text{bpy})_2^{2+} + e^- \rightarrow \text{Cu}^{\text{I}}(\text{bpy})_2^+$	0.1	2.0
$\text{Cu}^{\text{II}}(\text{OH})(\text{bpy})_2^+ + e^- \rightarrow \text{Cu}^{\text{I}}(\text{OH})(\text{bpy})_2$	-0.1	2.2
$\text{Cu}^{\text{II}}(\text{OAc})(\text{bpy})_2^+ + e^- \rightarrow \text{Cu}^{\text{I}}(\text{OAc})(\text{bpy})_2$	-0.1	2.2
$\text{tpy} - e^- \rightarrow \text{tpy}^{\bullet+}$	1.9	
$\text{Cu}^{\text{II}}(\text{tpy})_2^{2+} + e^- \rightarrow \text{Cu}^{\text{I}}(\text{tpy})_2^+$	-0.2	2.1
$\text{Cu}^{\text{I}}(\text{tpy})_2^+ + e^- \rightarrow \text{Cu} + 2\text{tpy}$	-0.9	2.8
$\text{PA}^- - e^- \rightarrow \text{PA}^{\bullet}$	1.3	
$\text{Cu}^{\text{II}}(\text{PA})_3^- + e^- \rightarrow \text{Cu}^{\text{I}}(\text{PA}) + 2\text{PA}^-$	-0.6	1.9
$\text{Cu}^{\text{I}}(\text{PA}) + e^- \rightarrow \text{Cu} + \text{PA}^-$	-1.6	2.9
$\text{AcO}^- - e^- \rightarrow \text{AcO}^{\bullet}$	1.2	
$\text{Cu}^{\text{I}}(\text{OAc})(\text{MeCN})_4 + e^- \rightarrow \text{Cu} + 4\text{MeCN} + \text{AcO}^-$	-1.2	2.4
$\text{Cu}^{\text{I}}(\text{OAc})(\text{bpy})_2 + e^- \rightarrow \text{Cu} + 2\text{bpy} + \text{AcO}^-$	-1.3	2.5
$\text{PhC(O)O}^- - e^- \rightarrow \text{PhC(O)O}^{\bullet}$	1.4	
$\text{Cu}^{\text{II}}[\text{OC(O)Ph}]_2 + e^- \rightarrow \text{Cu}^{\text{I}}[\text{OC(O)Ph}] + \text{PhC(O)O}^-$	-0.25	1.65
$\text{Cu}^{\text{I}}[\text{OC(O)Ph}] + e^- \rightarrow \text{Cu} + \text{PhC(O)O}^-$	-1.3	2.7
$\text{PhCH}_2\text{O}^- - e^- \rightarrow \text{PhCH}_2\text{O}^{\bullet}$	0.4	
$\text{Cu}^{\text{II}}(\text{OCH}_2\text{Ph})_2(\text{bpy})_2 - e^- \rightarrow \text{Cu}^{\text{I}}(\text{OCH}_2\text{Ph})_2 - (\text{bpy})_2$	-0.4	0.8
$\text{DPAH}^- - e^- \rightarrow \text{DPAH}^{\bullet}$	1.2	
$\text{Cu}^{\text{II}}(\text{DPAH})(\text{DPA})^- + e^- \rightarrow \text{Cu}^{\text{I}}(\text{DPA})^- + \text{DPAH}^-$	-0.5	1.7
$\text{DPA}^{2-} - e^- \rightarrow \text{DPAH}^{\bullet-}$	0.2	
$\text{Cu}^{\text{I}}(\text{DPA})^- + e^- \rightarrow \text{Cu} + \text{DPA}^{2-}$	-1.8	2.0
$\text{Cl}^- - e^- \rightarrow \text{Cl}^{\bullet}$	2.0	
$\text{Cu}^{\text{II}}\text{Cl}_2(\text{MeCN})_4 + e^- \rightarrow \text{Cu}^{\text{I}}\text{Cl}(\text{MeCN})_4 + \text{Cl}^-$	0.56	1.44
$\text{Cu}^{\text{II}}\text{Cl}_2(\text{bpy})_2 + e^- \rightarrow \text{Cu}^{\text{I}}\text{Cl}(\text{bpy})_2 + \text{Cl}^-$	0.02	1.98
$\text{Cu}^{\text{II}}\text{Cl}_2(\text{tpy}) + e^- \rightarrow \text{Cu}^{\text{I}}\text{Cl}(\text{tpy}) + \text{Cl}^-$	-0.1	2.1
$\text{Cu}^{\text{I}}\text{Cl}(\text{MeCN})_4 + e^- \rightarrow \text{Cu} + 4\text{MeCN} + \text{Cl}^-$	-1.2	3.2
$\text{Cu}^{\text{I}}\text{Cl}(\text{bpy})_2 + e^- \rightarrow \text{Cu} + 2\text{bpy} + \text{Cl}^-$	-1.25	3.25
$\text{Cu}^{\text{I}}\text{Cl}(\text{tpy}) + e^- \rightarrow \text{Cu} + \text{tpy} + \text{Cl}^-$	-1.15	3.15
$\text{HO}^- - e^- \rightarrow \text{HO}^{\bullet}$ (at pH 7 in H_2O)	2.1	
$\text{Cu}^{\text{I}}(\text{OH})(\text{H}_2\text{O})_3 + e^- \rightarrow \text{Cu} + 3\text{H}_2\text{O} + \text{HO}^-$	-0.3	2.4
$\text{Cu}^{\text{I}}(\text{OH})(\text{bpy})_2 + e^- \rightarrow \text{Cu} + 2\text{bpy} + \text{HO}^-$	-1.3	3.4

^a $E_{1/2}$ taken as $E_{p,a/2} + 0.03$ V for the irreversible reduction and $E_{p,c/2} - 0.03$ V for the irreversible oxidation.

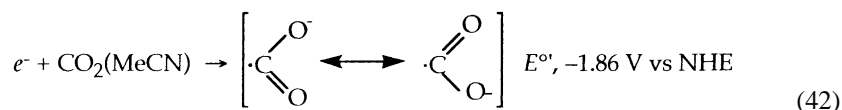
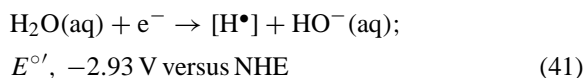
^b Saturated calomel electrode (SCE) vs. NHE, +0.244 V.

^c $\Delta E = E_{1/2(\text{L}^+/ \text{L})} - E_{1/2(\text{Cu}^{\text{II}}/\text{Cu}^{\text{I}})}$ or $\Delta E = E_{1/2(\text{L}^+/ \text{L})} - E_{1/2(\text{Cu}^{\text{I}}/\text{Cu})}$.

4. Reductive electrochemistry

The free electron interacts with all atoms and molecules that have finite electron affinities to produce anions, and thus is unstable in all but the most

inert liquids. Electrochemistry attests to this general axiom and provides a convenient means to evaluate the energetics for the addition of an electron to sol-



vent molecules and to species within a solution [1], e.g.

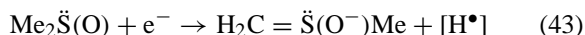


Table 7
Apparent metal–ligand covalent bond-formation free energies ($-\Delta G_{BF}$) for several copper complexes

Metal–ligand bond	$-\Delta G_{BF}$ (kcal mol ⁻¹)
(bpy) ⁺ –Cu ^{II} (bpy) ₂ ⁺	46
(bpy) ⁺ –Cu ^{II} (OH)(bpy)	51
(bpy) ⁺ –Cu ^{II} (OAc)(bpy)	51
(tpy) ⁺ –Cu ^{II} (tpy) ⁺	48
(tpy) ⁺ –Cu ^I (tpy)	64
PA–Cu ^{II} (PA) ₂ ⁻	43
PA–Cu ^I	67
AcO–Cu ^I (MeCN) ₄	55
AcO–Cu ^I (bpy) ₂	57
PhC(O)O–Cu ^{II} [OC(O)Ph]	37
PhC(O)O–Cu ^I	62
PhCH ₂ O–Cu ^{II} (OCH ₂ Ph)(bpy) ₂	18
DPAH–Cu ^{II} (DPA) ⁻	39
DPA–Cu ^I	46
Cl–Cu ^{II} Cl(MeCN) ₄	33
Cl–Cu ^{II} Cl(bpy) ₂	46
Cl–Cu ^{II} Cl(tpy)	48
Cl–Cu ^I (MeCN) ₄	74
Cl–Cu ^I (bpy) ₂	75
Cl–Cu ^I (tpy)	73
HO–Cu ^I (H ₂ O) ₃	55
HO–Cu ^I (bpy) ₂	78

Table 8
Electrochemical oxidation potentials for M^{II}(TDT)₂²⁻ complexes in MeCN (0.1 M TEAP)

Metal (M)	$E_{p,a}$ (V vs. SCE)		$-\Delta G_{BF}$ (kcal mol ⁻¹)	
	First oxidation	Second oxidation	M ^{III} –S	M ^{IV} –S
TDTH ⁻	-0.05 (irreversible)			
Zn	+0.18 (irreversible)			
Cu	-0.53	+0.62	16.4	
Ni	-0.47	+0.44	15.0	4.2
Co	-0.73	+0.20	21.0	9.7
Fe	-0.83	+0.10, +0.32	23.3	12.0
Mn	-0.63	+0.22 (irreversible)	18.7	9.2

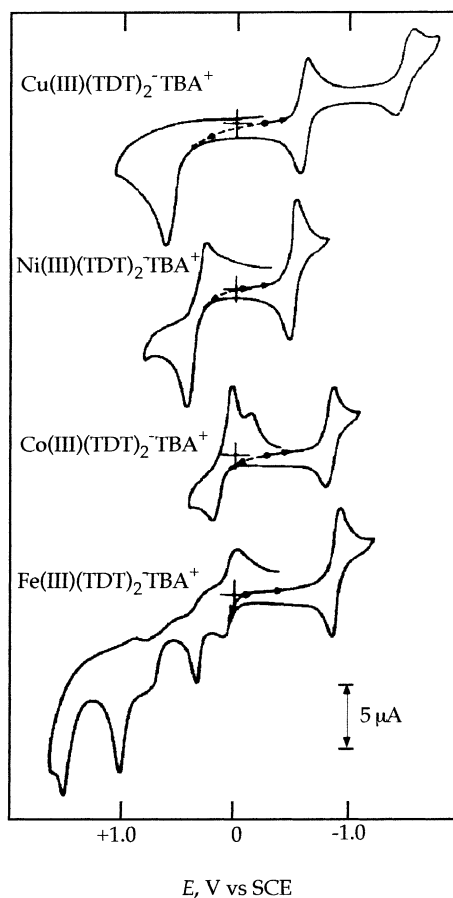
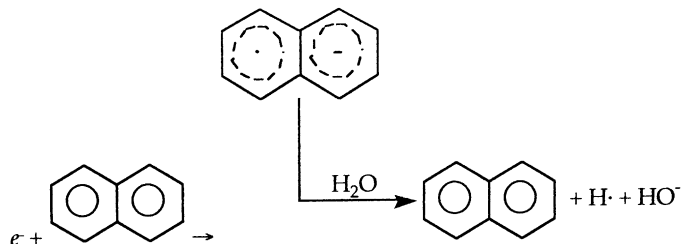


Fig. 4. Cyclic voltammograms in MeCN (0.1 M TEAP) of 1 mM [M^{III}(TDT)₂](Bu₄N) complexes (M = Cu, Ni, Co, and Fe; TDT, toluene dithiolate). Scan rate 0.1 V s⁻¹; Pt electrode area = 0.11 cm².

Hence, reductive electrochemistry converts electrons (e^-) via the solution matrix at the interface to atoms and anions. The solution outside the inner double layer *never* is exposed to an electron. Some examples of such *inner-double-layer electron transfer*

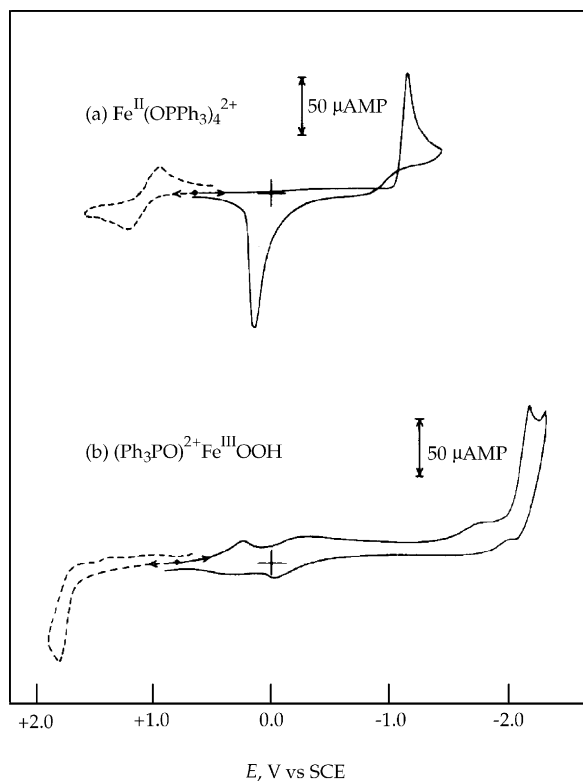
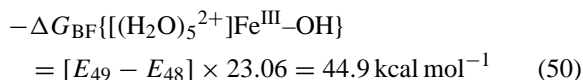
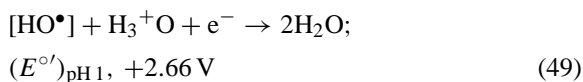
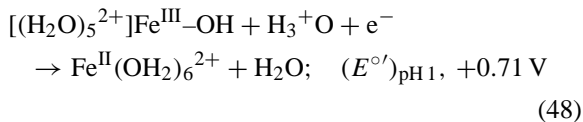
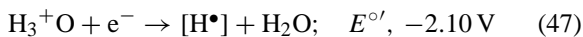
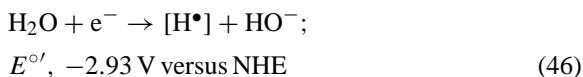
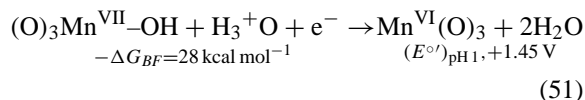


Fig. 5. Cyclic voltammograms in MeCN for: (a) 3 mM $\text{Fe}^{\text{II}}(\text{OPPh}_3)_4(\text{ClO}_4)_2$; (b) 3 mM $\{[(\text{Ph}_3\text{PO})_4]^{2+}\text{Fe}^{\text{III}}(\text{OOH})\}(\text{ClO}_4^-)_2$. Scan rate 0.1 V s^{-1} ; glassy-carbon working electrode (area = 0.11 cm^2).

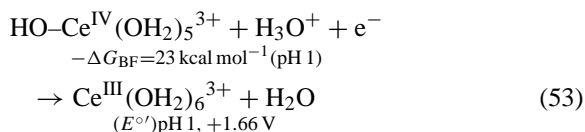
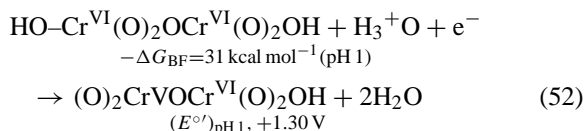
include:



The electrochemical reduction of permanganic acid [$\text{HMn}^{\text{VII}}(\text{O})_3$], which is traditionally represented as a metal-centered electron transfer to change Mn^{7+} to Mn^{6+} , is another example of a ligand-centered process

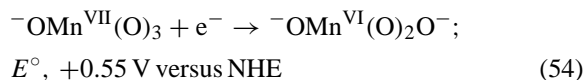


Comparison of this with the reduction of free hydroxyl radical (HO^\bullet) (Eq. (49)) provides a measure of the $\text{HO-Mn}^{\text{VII}}(\text{O})_3$ bond energy [$-\Delta G_{\text{BF}} = (2.66 - 1.45) \times 23.06 = 28 \text{ kcal mol}^{-1}$]. The other strong oxidants [$(\text{HO})_2\text{Cr}_2^{\text{VI}}(\text{O})_5$ and $\text{HO}\text{Ce}^{\text{IV}}(\text{OH}_2)_5^{3+}$] that are used for aqueous redox titrations are reduced by a similar path



An important point in these electron-transfer reductions is that the primary electron acceptor is the hydronium ion (H_3^+O), which is transformed to a hydrogen atom (H^\bullet) that reacts with HO^\bullet (either free or bound via a covalent bond to the metal center). Thus, in the reactions of Eqs. (48), (49), and (51)–(53), the oxidant in each is the hydronium ion (H_3^+O) and the reduction potential is determined by the H–OH bond energy ($-\Delta G_{\text{BF}}$) of the product H_2O , minus the metal–OH bond energy (Eqs. (51)–(53)).

Under alkaline conditions $\text{Mn}^{\text{VII}}\text{O}_4^-$ is reduced via direct electron addition to one of the bound oxygen atoms



The extent of the stabilization of the oxygen atom in $\text{Mn}^{\text{VII}}\text{O}_4^-$ is indicated by the reduction potential for a free $\bullet\text{O}^\bullet$ atom

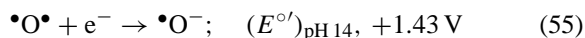


Table 9

Redox potentials for (Cl₈TPP)M porphyrins (M = Zn, Mn, Fe, Co), and their complexes in H₂CCl₂

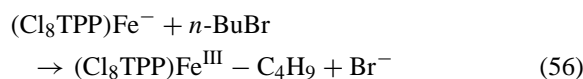
	$(E^\circ)'$ (V vs. SCE)				
	MP ²⁺ ← MP ^{•+}	MP ^{•+} ← MP	PML ← PM ⁺ L ⁻	MP → MP ^{•-}	MP ^{•-} → MP ²⁻
(Cl ₈ TPP)H ₂	+1.63	+1.23		-1.10	-1.54
(Cl ₈ TPP)Zn ^{II}	+1.34	+1.02		-1.27	-1.72
(Cl ₈ TPP)Mn ^{III} Cl ^a	+1.49	-0.06	-0.23	-1.34	
(Cl ₈ TPP)Fe ^{III} Cl	+1.64	+1.35	-0.29	-0.97 (M → M ⁻)	-1.63
(Cl ₈ TPP)Co ^{II}	+1.25	+0.82		-0.86 (M → M ⁻)	-1.29
(Cl ₈ TPP)Fe ^{III} OH ^b	+1.64	+1.35	-0.75	-1.31	-1.63

^a (Cl₈TPP)Mn^{III}Cl → [(Cl₈TPP)Mn^{IV}Cl]⁺ + e⁻, $(E^\circ)' = +0.88$ V vs. SCE.

^b (Cl₈TPP)Fe^{III}OH → [(Cl₈TPP)Fe^{IV}(O)] + e⁻, $(E^\circ)' = +1.00$ V vs. SCE; generated from (Cl₈TPP)Fe^{III}Cl + 1 eq. of (Bu₄N)OH.

5. Metalloporphyrins

Although metallo-porphyrins often are classified as coordination complexes, they are much closer to organometallic compounds with their strong metal–nitrogen covalent bonds. Table 9 summarizes the redox potentials for several neutral porphyrins and their chloro and hydroxo derivatives [6]. Again, the electron-transfer processes are ligand or porphyrin centered. However, the reductions of (Cl₈TPP)Co^{II} and (Cl₈TPP)Fe^{II} are unique because they are metal-centered to give (Cl₈TPP)Co⁻ and (Cl₈TPP)Fe⁻ [11]. The latter are nucleophiles that react with alkyl halides, e.g.



6. Organometallic molecules

The defining characteristic of organometallic molecules is the presence of one or more metal–carbon bonds. In contrast to the acid/base character of coordination complexes of metal ions (with their ligand-centered redox chemistry), the metal–carbon center is highly covalent with limited polarity (similar to carbon–carbon, carbon–nitrogen, or carbon–oxygen centers). As a result, the electrochemistry of organometallic molecules is more closely related to that of organic molecules than inorganic coordination complexes.

The “foundation stone” of organometallic chemistry is bis(cyclopentadienyl) iron(II) [ferrocene,

(Cp)Fe^{II}(Cp)], an iron atom sandwiched between two five-membered carbon rings [Cp, C₅H₅[•]; each carbon with a p electron to give (a) two pi-bonds delocalized around the carbon ring and (b) an unpaired electron that is shared by the five carbons of the ring]. Thus, the Fe^{II}(Cp)₂ molecule has the iron on a line that connects the centers of two parallel planar Cp[•] groups to give an “iron sandwich”.

Fig. 6 illustrates the electrochemical redox chemistry in acetonitrile for several coordination complexes of iron [Fe^{II}(MeCN)₄²⁺, Fe^{III}Cl₃, and Fe^{III}(acac)₃ (acac = acetylacetonate)] in relation to that for two iron organometallics [Fe^{II}(Cp)₂ and Fe(CO)₅ (iron-pentacarbonyl); both stable 18-electron systems] [12]. In MeCN Fe^{II}(MeCN)₄²⁺ is the only charged species of the group. It is reversibly oxidized (II/III couple; $E_{1/2}$, +1.6 V versus SCE). The uncharged Fe^{III}Cl₃ molecule is reversibly reduced (III/II couple; $E_{1/2}$, +0.2 V versus SCE) to give Fe^{II}Cl₃⁻, which is reduced by an irreversible two-electron process to iron metal ($E_{p,c}$, -1.5 V versus SCE). The more basic Fe^{III}(acac)₃ molecule is reversibly reduced (III/II couple; $E_{1/2}$, -0.7 V versus SCE), but does not exhibit a second reduction peak. The III/II reduction potentials for these three coordination complexes are a measure of their relative electrophilicity (Lewis acidity).

7. Ferrocene

The Fe^{II}(Cp)₂ molecule is resistant to reduction, but exhibits a highly reversible one-electron oxidation

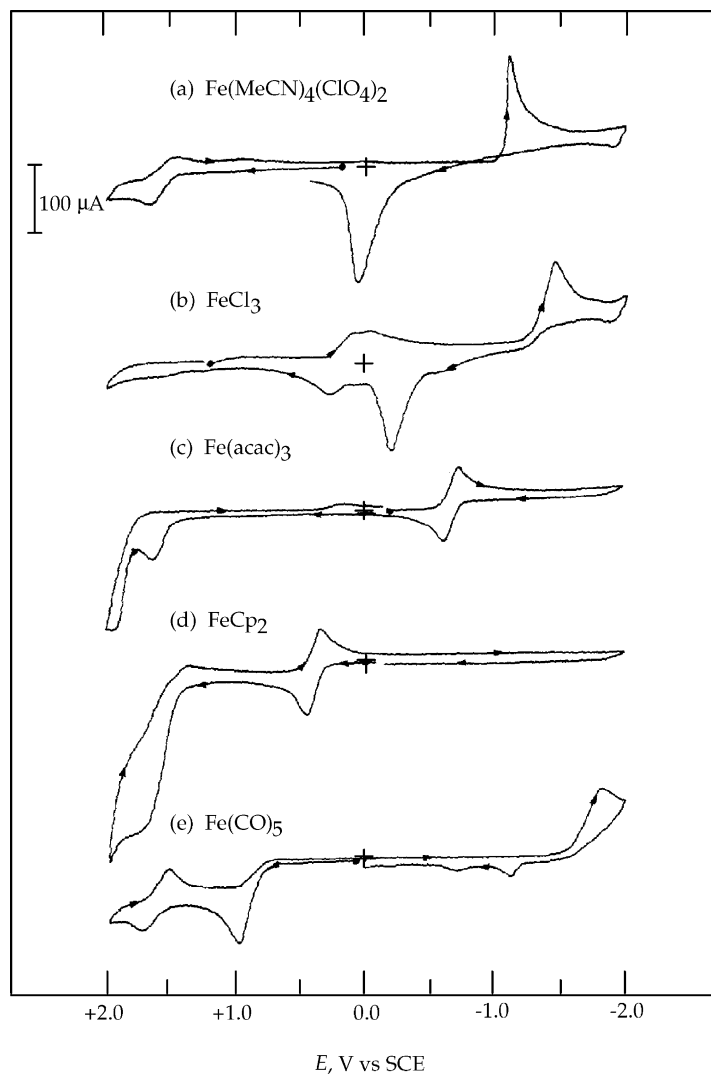
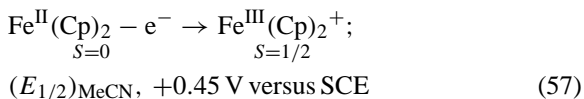


Fig. 6. Cyclic voltammograms: (a) 3 mM $[\text{Fe}^{\text{II}}(\text{MeCN})_4](\text{ClO}_4)_2$; (b) 3 mM $\text{Fe}^{\text{III}}\text{Cl}_3$; (c) 3 mM $\text{Fe}^{\text{III}}(\text{acac})_3$; (d) 3 mM $\text{Fe}^{\text{II}}(\text{Cp})_2$; (e) 3 mM $\text{Fe}^{\text{V}}(\text{CO})_5$ in MeCN (0.1 M tetraethylammonium perchlorate (TEAP)). Conditions: scan rate 0.1 V s^{-1} ; ambient temperature; glassy-carbon working electrode (area = 0.09 cm^2); saturated calomel electrode (SCE) vs. NHE, $+0.244 \text{ V}$.

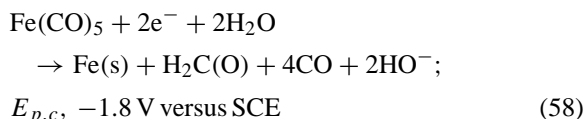


with the single positive charge delocalized over the 10 equivalent (Cp)₂ hydrogens (+0.1 each). For a time there was a belief that the $\text{Fe}^{\text{II}}(\text{Cp})_2/\text{Fe}^{\text{III}}(\text{Cp})_2^+$ couple's potential was independent of solvent, and thus an ideal reference electrode with which to mea-

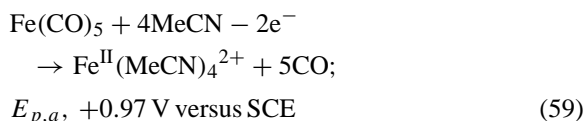
sure solvent effects for other redox couples. However, subsequent measurements have shown that the $\text{Fe}^{\text{III}}(\text{Cp})_2^+$ ion possesses considerable acidity, which causes some solvent effects. The more serious problem is the limited solubility of $\text{Fe}^{\text{II}}(\text{Cp})_2$ in H_2O . The respective E'° values for the $\text{Fe}^{\text{III}}(\text{Cp})_2^+/\text{Fe}^{\text{II}}(\text{Cp})_2$ couple are: MeCN, $+0.69 \text{ V}$ versus NHE ($+0.45 \text{ V}$ versus SCE); DMF, $+0.72 \text{ V}$; py, $+0.76 \text{ V}$; Me_2SO , $+0.68 \text{ V}$; H_2O , $+0.40 \text{ V}$ [13].

8. Iron-pentacarbonyl

The $\text{Fe}(\text{CO})_5$ molecule is equally fundamental to organometallic chemistry and electrochemistry, and like $\text{Fe}^{\text{II}}(\text{Cp})_2$ is a diamagnetic 18-electron system. It exhibits (a) an irreversible two-electron oxidation (Fig. 6e) [12]. In each case, $\text{Fe}(\text{CO})_5$ has a synergistic effect on (a) the reduction of residual H_2O and (b) the oxidation of solvent molecules.



By an analogous process, the CO adduct of an iron(II) porphyrin [$(\text{Cl}_8\text{TPP})\text{Fe}^{\text{IV}}(\text{CO})$] is reduced to $\text{H}_2\text{C}(\text{O})$ at -0.87 V [14]. The oxidation of $\text{Fe}(\text{CO})_5$ in MeCN yields $\text{Fe}^{\text{II}}(\text{MeCN})_4^{2+}$ in a two-electron process (Fig. 6e)



On the basis that $\text{Fe}(\text{s})$ is oxidized to $\text{Fe}^{\text{II}}(\text{MeCN})_4^{2+}$ at $\sim 0.0 \text{ V}$ (Fig. 6e), the carbonyls of $\text{Fe}(\text{CO})_5$ stabilize the iron against oxidation by about 45 kcal mol^{-1} [$2 \times \Delta E \times 23.06 \text{ kcal mol}^{-1} (\text{eV})^{-1}$; $2 \times 0.97 \times 23.06$]. The $(\text{Cl}_8\text{TPP})\text{Fe}^{\text{IV}}(\text{CO})$ molecule is oxidized at $+0.75 \text{ V}$ versus $+0.32 \text{ V}$ for $(\text{Cl}_8\text{TPP})\text{Fe}^{\text{II}}$; a stabilization by the CO of about 10 kcal mol^{-1} [14].

These examples of the electrochemical character of organometallics are limited, but illustrate that their oxidation and reduction is closely similar to that for organic molecules. Thus, electron-transfer is never carbon-centered, and often involves residual water [H-atom addition via reduction and (HO^\bullet) addition or H-atom abstractron via oxidation] or solvent components.

In summary, the electron-transfer reactions for metals, metal complexes, and metalloporphyrins are ligand-centered (or solvent-centered). In each case, the potential for the oxidation of free ligand is decreased in the presence of metal or reduced-metal complex by an amount that is proportional to the

metal–ligand bond energy ($-\Delta G_{\text{BF}}$). The role of the metal center is to facilitate electron removal from the Lewis-base ligand via covalent bond formation [e.g. $\text{Ag}(\text{s}) + 6\text{H}_2\text{O} - e^- \rightarrow \text{Ag}^{\text{I}}(\text{OH}_2)_6^+$ ($E^\circ = +0.80 \text{ V}$ versus NHE; $-\Delta G_{\text{BF}} = 105 \text{ kcal mol}^{-1}$); $\text{Ag}(\text{s}) + \text{Cl}^- - e^- \rightarrow \text{Ag}^{\text{I}}\text{Cl}(\text{s})$ ($E^\circ = +0.22 \text{ V}$; $-\Delta G_{\text{BF}} = 120 \text{ kcal mol}^{-1}$)]. The greater covalent bond energy for $\text{Ag}^{\text{I}}\text{–Cl}$ accounts for its formation via nucleophilic substitution [$\text{Cl}^- + \text{Ag}^{\text{I}}(\text{OH}_2)_6^+ \rightarrow \text{Ag}^{\text{I}}\text{Cl}(\text{s}) + 6\text{H}_2\text{O}$]. This is more reasonable than the traditional electrostatic ionic-bond formulation; especially when it is realized that the hydrated ionic radius of sodium ion and silver ion are the same.

Acknowledgements

This work has been supported by the Provost's Office of Texas A&M University.

References

- [1] D.T. Sawyer, A. Sobkowiak, J.L. Roberts Jr., *Electrochemistry for Chemists*, 2nd ed., Wiley/Interscience, New York, 1995.
- [2] D.R. Lide (Ed.), *CRC Handbook of Chemistry and Physics*, vol. 10, 74th ed., CRC Press, Boca Raton, FL, 1993, pp. 180–181, 205–207.
- [3] D.R. Lide (Ed.), *CRC Handbook of Chemistry and Physics*, vol. 9, 74th ed., CRC Press, Boca Raton, FL, 1993, pp. 123–141.
- [4] A.J. Bard, R. Parsons, J. Jordan (Eds.) *Standard Potentials in Aqueous Solution*, Marcel Dekker, New York, 1985.
- [5] D.T. Sawyer, P. Chooto, P.K.S. Tsang, *Langmuir* 5 (1989) 84.
- [6] S.A. Richert, P.K.S. Tsang, D.T. Sawyer, *Inorg. Chem.* 28 (1989) 2471.
- [7] A. Sobkowiak, A. Qiu, A. Llobet, D.T. Sawyer, *J. Am. Chem. Soc.* 115 (1993) 609.
- [8] A. Qiu, Ph.D. Dissertation, Texas A&M University, College Station, TX, 1992.
- [9] D.T. Sawyer, G.S. Srivatsa, M.E. Bodini, W.P. Schaefer, R.M. Wing, *J. Am. Chem. Soc.* 108 (1986) 936.
- [10] D.T. Sawyer, M.S. McDowell, L. Spencer, P.K.S. Tsang, *Inorg. Chem.* 28 (1989) 1166.
- [11] A. Qiu, D.T. Sawyer, *J. Porph. Phthal.* 1 (1997) 125–134.
- [12] S.A. Richert, Ph.D. Dissertation, Texas A&M University, College Station, TX, 1989, pp. 49–53.
- [13] W.C. Barrette Jr., H.W. Johnson Jr., D.T. Sawyer, *Anal. Chem.* 56 (1984) 1890.
- [14] H.-C. Tung, P. Chooto, D.T. Sawyer, *Langmuir* 7 (1991) 1635.